

Synthesis and characterization of p-type transparent conducting CuAlO_2 thin film by DC sputtering

A.N. Banerjee, S. Kundoo, K.K. Chattopadhyay*

Department of Physics, Jadavpur University, Calcutta 700 032, India

Received 9 May 2002; received in revised form 15 April 2003; accepted 23 April 2003

Abstract

P-type transparent conducting thin films of copper aluminium oxide were prepared by DC sputtering of polycrystalline CuAlO_2 target, which was fabricated by heating a stoichiometric mixture of Cu_2O and Al_2O_3 at 1375 K for 24 h. Thin films of CuAlO_2 were deposited on Si (4 0 0) and glass substrates. The sputtering was performed in $\text{Ar} + \text{O}_2$ (40 vol.%) atmosphere and the substrate temperature was 453 K. X-ray diffraction spectra of the films showed the peaks that could be assigned with those of the crystalline CuAlO_2 . Fourier transform infrared spectra showed Cu–O, Al–O, O–Cu–O bonding. UV–Vis–NIR spectrophotometric measurement showed high transparency of the films in the visible region. Both direct and indirect band gaps were found to exist and their corresponding estimated values were 3.66 and 2.1 eV, respectively. The room temperature conductivity of the film was fairly high and was of the order of 0.08 S cm^{-1} , while the activation energy was $\sim 0.26 \text{ eV}$. Thermoelectric power measurement indicated positive value of Seebeck coefficient and its room temperature value was $+128 \mu\text{V K}^{-1}$. Positive value of Hall coefficient ($R_H = +16.7 \text{ cm}^3 \text{ C}^{-1}$) also confirmed p-type conductivity of the films.

© 2003 Elsevier Science B.V. All rights reserved.

Keywords: Copper aluminium oxide; Sputtering; Transparent; P-type conductivity

1. Introduction

Doped versions of transparent conducting oxides (TCOs) such as ZnO_{1-x} , $\text{In}_{1-x}\text{Sn}_x\text{O}_3$, $\text{SnO}_2:F$, Cd_2SnO_4 , etc. are all n-type materials, which are widely used as transparent electrodes in flat panel displays, as window layers in solar cells and in many such applications [1–4]. But there are very few reports on p-type TCOs until Kawazoe et al. [5] reported p-type conductivity in a transparent thin film of copper aluminium oxide (CuAlO_2). In fact, delafossite $\text{Cu}^I\text{M}^{\text{III}}\text{O}_2$ class of materials, where M^{III} is a trivalent cation, have recently attracted great attention of various researchers around the globe, because it fueled the hopes that transparent electronics might be feasible [6–10]. For example, a combination of the two types of TCOs in the form of a p–n junction could lead to a ‘functional’ window, which transmits visible portion of solar radiation yet generates electricity by the absorption of the UV part of it. Apart from these, it can also be used as a good thermoelectric

material [11]. Combining all these properties, CuAlO_2 became an important material in the last few years and attracted attention of many researchers.

Recently, various research groups are working on the synthesis of several p-type transparent conducting oxide thin films and also on device fabrications using them. Kudo et al. [12] reported the synthesis of wide band gap p-type SrCu_2O_2 thin films on SiO_2 glass substrates by pulsed laser deposition (PLD). Fabrication of p–n heterojunction diode using n-ZnO/p- SrCu_2O_2 was also reported by them [13]. Kawazoe et al. recently reported synthesis of different p-type conducting oxides like CuAlO_2 , CuGaO_2 , SrCu_2O_2 and also p–n heterojunction fabrication with other n-type transparent oxides [14]. Infrared transparent spinel films such as NiCo_2O_4 with p-type conductivity was reported by Windisch et al. [15,16].

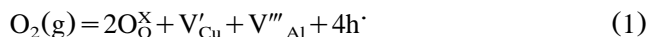
Structure of CuAlO_2 delafossite had been extensively studied by Ishiguro et al. [17], where they proposed an alternative stacking of Cu^I and layers of nominal AlO_2 composition consisting of Al– O_6 octahedra sharing edges. Each Cu atom is linearly coordinated with two

*Corresponding author. Tel.: +91-33-473-4044.

E-mail address: kkc@juphys.ernet.in (K.K. Chattopadhyay).

oxygen atoms to form a O–Cu–O dumbbell unit placed parallel to the *c*-axis. O-atoms of O–Cu–O dumbbell link all Cu layers with the AlO₂ layers.

The cause of p-type conductivity shown by this material is due to metal deficit (or excess oxygen) within the crystallite sites of the material, i.e. the defect chemistry plays an important role. This is due to the deviation from the stoichiometric composition of the components, which can be induced by regulating the preparation condition of the material. The defect reaction may be represented by the following equation [18]:



where O_O, V_{Cu}, V_{Al} and h denote lattice oxygen, Cu vacancy, Al vacancy and hole, respectively. Superscripts X, ' and · denote effective neutral, negative and positive charge states, respectively.

For the synthesis of CuAlO₂ thin films, Kawazoe et al. [5] and Yanagi et al. [19] used PLD method. However, there are some limitations of the PLD method such as the necessity of costly equipment and the difficulty in scaling-up of the technology. Hence, it is of utmost importance to develop alternative synthesis route of this important material for the full exploitation of its tremendous technological potential. In this article, we report synthesis and characterization of this material by DC sputtering. We preferred sputtering over other methods because large-area deposition is possible by this technique. Also complex shaped substrates can be coated conveniently by this process and it is cost-effective.

2. Experiments

2.1. Powder preparation

Polycrystalline CuAlO₂ powder was synthesized by heating stoichiometric mixture of Cu₂O and Al₂O₃. At first, Cu₂O and Al₂O₃ powder (99.99%) were taken with Cu/Al atomic ratio 1:1 and mixed for 1 h. Then, the mixture was heated in alumina boat at 1100 °C for 24 h. In every 6 h, the mixture was taken out of the furnace after proper cooling, remixed and placed into the furnace at the same temperature. The sintered body was reground and pressed into pellets by hydrostatic pressure of approximately 200 kgf cm⁻². These pellets were placed in aluminium holder by some appropriate arrangement, which was used as the target for sputtering.

2.2. Film deposition

Our sputtering system consists of a conventional vacuum system, which was evacuated to 10⁻⁶ mbar by rotary and diffusion pump arrangement. The chamber was back filled with Ar and O₂ (40 vol.%) gas mixture.

Table 1
Summary of deposition parameters

Electrode distance	1.8 cm
Sputtering voltage	1.1 kV
Current density	10 mA cm ⁻²
Substrates	Si (4 0 0), glass
Sputtering gasses	Ar and O ₂ (3:2 volume ratio)
Deposition pressure	0.2 mbar
Substrate temperature	453 K
Deposition time	4 h

The target was pre-sputtered for 10 min to remove contamination, if any, from the surface and then the shutter was displaced to expose the substrates in the sputtering plasma. Si (4 0 0) and glass were used as substrates. Before placing into the deposition chamber, the glass substrates were cleaned at first by mild soap solution, then washed thoroughly in deionized water and also in boiling water. Finally, they were ultrasonically cleaned in acetone for 15 min. Si substrates were immersed in 20% HF solution for 5 min for removing surface oxide layers. Then they were cleaned in deionized water and finally with alcohol in an ultrasonic cleaner. The summary of deposition conditions is shown in Table 1. After the deposition was over, the films were post-annealed in the same vacuum chamber at 473 K for 1 h (at pressure 0.2 mbar), maintaining the oxygen flow.

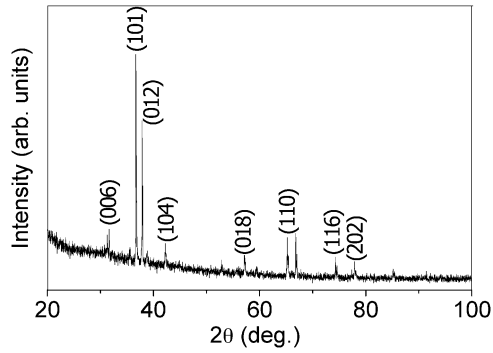
2.3. Characterization

The deposited films were characterized by X-ray diffraction (XRD, by Cu Kα line), scanning electron microscopy (JEOL-5200) and Fourier transform infrared spectroscopy (FTIR, NICOLET MAGNA-750) studies to investigate the film morphology and structural properties. Optical transmittance and reflectance were measured by a UV–Vis–NIR spectrophotometer (HITA-CHI-U3410). Thermoelectric power (TEP) and Hall effect study were used to determine the type of conduction taking place in the deposited films. Temperature dependence of electrical conductivity of the films was studied by standard four-probe method. The contact was made with silver paint, which showed linear *I*–*V* characteristic over a wide range of applied voltage.

3. Results and discussion

3.1. Structural properties

Fig. 1 shows the XRD pattern of the synthesized CuAlO₂ powder, which was used for target preparation. The peaks of the powdered material are identified to originate from (0 0 6), (1 0 1), (0 1 2), (1 0 4), (0 1 8), (1 1 0), (1 1 6) and (2 0 2) reflections. This pattern closely reflects the rhombohedral crystal structure with

Fig. 1. XRD pattern of CuAlO_2 powder.

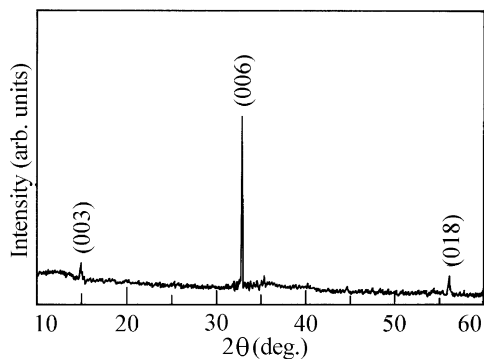
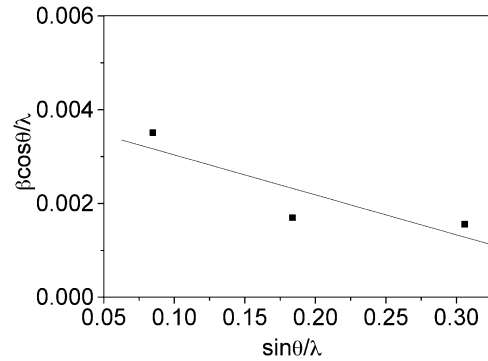
R3m space group [20]. Fig. 2 shows XRD pattern of the as-deposited thin film on Si substrate. The XRD pattern shows a strong (0 0 6) orientation. Similar orientation was also observed by Kawazoe and Yanagi et al. [5,19], for their CuAlO_2 films deposited on sapphire substrates. Also, no peaks of starting materials (e.g. Cu_2O and Al_2O_3) have been found, which conclusively indicates that the reactants were completely mixed to form the new phase of copper aluminium oxide.

The information on strain and the particle size of the deposited films could be obtained from the full-width-at-half-maximum (FWHM) of the diffraction peaks. The FWHM's (β 's) can be expressed as a linear combination of the contributions from the strain (ε) and the particle size (L) through the following relation [21]:

$$\beta \cos \theta / \lambda = 1/L + \varepsilon \sin \theta / \lambda \quad (2)$$

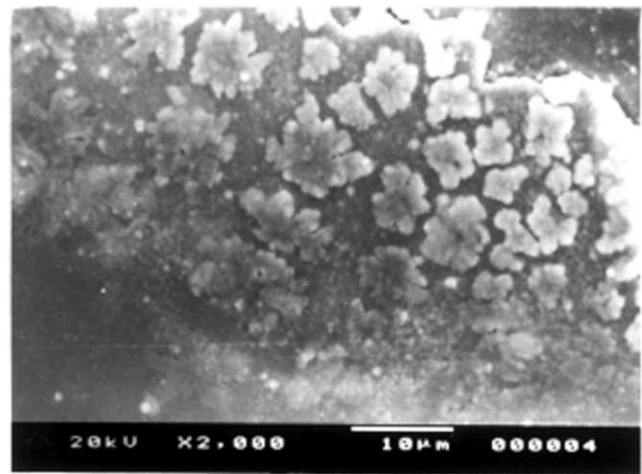
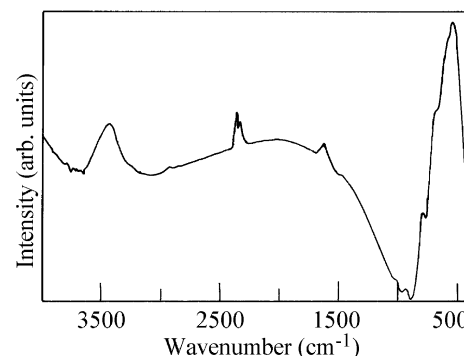
Fig. 3 represents the plot of $\beta \cos \theta / \lambda$ vs. $\sin \theta / \lambda$. Slope of the graph depicts the strain value as 8.52×10^{-3} and the intercept on y-axis gives the particle size as ~ 26 nm.

Fig. 4 shows the scanning electron micrograph of a typical CuAlO_2 film deposited on Si substrate. Very fine grains could be observed from the micrograph, the size of which is difficult to measure accurately from the

Fig. 2. XRD pattern of CuAlO_2 thin film deposited on Si (4 0 0) substrate.Fig. 3. Plot to determine strain and particle size of CuAlO_2 thin film deposited on Si substrate.

micrograph. Some bigger clusters are also observed, which was the result of agglomeration of finer grains. From the cross-sectional SEM image (not shown here), thickness of the film was determined to be $\sim 0.7 \mu\text{m}$.

Fig. 5 represents the FTIR spectra of the CuAlO_2 films deposited on Si substrates. All bands have been

Fig. 4. SEM photograph of a CuAlO_2 thin film deposited on Si substrate.Fig. 5. FTIR spectrum of CuAlO_2 thin film on Si substrate.

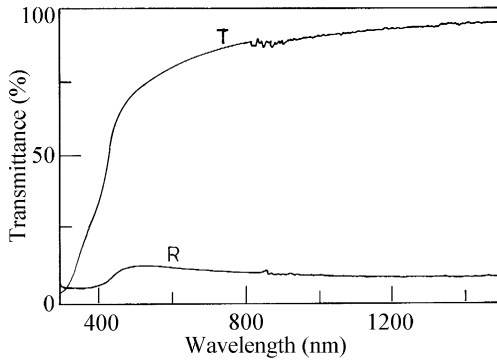


Fig. 6. Optical transmittance and reflectance spectra of CuAlO₂ thin film deposited on glass substrate.

assigned to the absorption peaks of Cu–O, O–Cu–O, Al–O bond vibrations. The broad peak ranging from 500 to 900 cm⁻¹ is actually consisting of a number of peaks, which can be obtained by deconvoluting the peak. The absorption peaks near 550 and 600 cm⁻¹ may be assigned to be due to Cu–O stretching vibration and O–Cu–O antisymmetric vibration, respectively. The peak approximately 600 cm⁻¹ originates owing to Al–O stretching vibration in AlO₆ octahedra of CuAlO₂ structure. Peaks ranging from 700 to 900 cm⁻¹ may be assigned to be due to short Al–O stretching vibrations in distorted AlO₆ octahedra. Peak approximately 1000 cm⁻¹ may be assigned to Si–O–Al vibration that occurs because of Si substrate used [22,23]. Peak at 2349 cm⁻¹ is a CO₂ peak and the broad peak approximately 3000–3500 cm⁻¹ is due to O–H stretching vibration, which may be incorporated from the atmospheric contamination. From the literature survey, it becomes clear that there is no reported study on FTIR of the CuAlO₂. So, there may remain some unidentified peaks such as approximately 1633 cm⁻¹ in our FTIR spectra. Proper identification of all the peaks may become further topic of research for clear understanding of the electro–opto properties of this as well as similar kind of TCOs.

3.2. Optical properties

The optical transmittance spectrum of the CuAlO₂ thin films deposited on glass substrates were recorded from 300 nm to 1500 nm wavelength range taking similar glass as reference, and hence the spectrum gives transmittance of the films only. Reflectance of films was also measured over the same wavelength range. Fig. 6 shows the transmittance and reflectance vs. wavelength plots of a typical CuAlO₂ thin film. With the known film thickness as measured from the cross-sectional SEM micrograph, absorption coefficients were determined using the formula given by Demichelis et al. [24]. Fig. 7 shows the variation of the absorption coefficient with wavelength over the measured region.

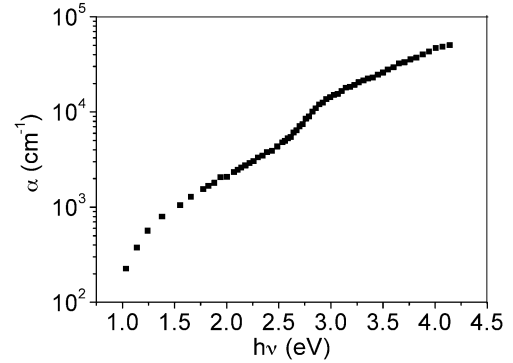


Fig. 7. Variation of absorption coefficient with wavelength.

The fundamental absorption, which corresponds to electron excitation from the valance band to conduction band, can be used to determine the nature and value of the optical band gap. The relation between the absorption coefficients (α) and the incident photon energy ($h\nu$) can be written as [25]

$$(\alpha h\nu)^{1/n} = A(h\nu - E_g) \quad (3)$$

where A is a constant and E_g is the band gap of the material and exponent n depends on the type of transition. For direct allowed, $n=1/2$, for indirect allowed transition, $n=2$, and for direct forbidden, $n=3/2$. To determine the possible transitions, $(\alpha h\nu)^{1/n}$ vs. $h\nu$ were plotted for different values of n . The $(\alpha h\nu)^2$ vs. $h\nu$ plots is shown in Fig. 8. Extrapolating the linear portion of the graph to the $h\nu$ -axis, we have obtained the direct band gap from the intercept on $h\nu$ -axis, which comes out to be ~ 3.66 eV. The inset of Fig. 8 shows $(\alpha h\nu)^{1/2}$ vs. $h\nu$ plots and the indirect band gap comes out as ~ 2.1 eV. These values nearly agree with the values reported by Kawazoe et al. [5] for their PLD deposited films.

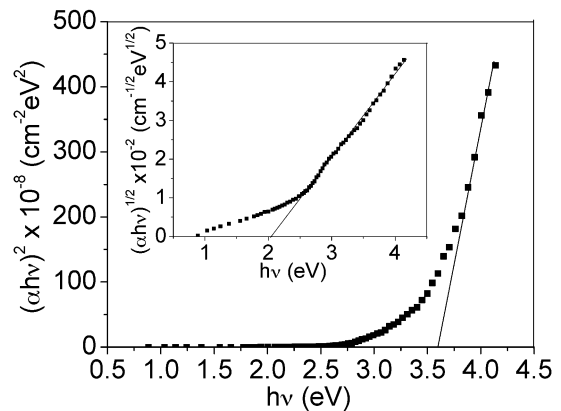


Fig. 8. Plot to test for direct allowed transition for CuAlO₂ thin film. Inset: determination of indirect band gap.

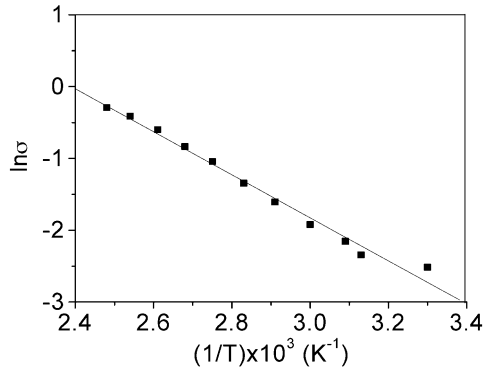


Fig. 9. Temperature dependence of electrical conductivity of CuAlO₂ thin film.

3.3. Electrical properties

Fig. 9 represents $\ln \sigma$ vs. $1/T$ plot of the CuAlO₂ film on glass substrate from room temperature (300 K) to 575 K. The temperature variation of conductivity of the CuAlO₂ thin films was studied below the room temperature by previous authors [5,19], but no study in the temperature range higher than room temperature was reported. The straight-line nature of the Arrhenius plot indicates the thermally activated conduction, as often found in semiconductors. Room temperature conductivity of the film was obtained as 0.08 S cm^{-1} , which is comparable with that obtained by Kawazoe et al. [5]. From the slope of the graph, we get the value of activation energy (E_a), which corresponds to the minimum energy required to transfer carriers from acceptor level to the valence band and the value of E_a comes out as 0.26 eV.

TEP of the CuAlO₂ thin films deposited on glass substrates was measured over the temperature range 300–500 K. Fig. 10 shows the variation of the Seebeck coefficient with temperature for a typical CuAlO₂ thin film and the positive value of the Seebeck coefficient indicates p-type nature of the films. Room temperature

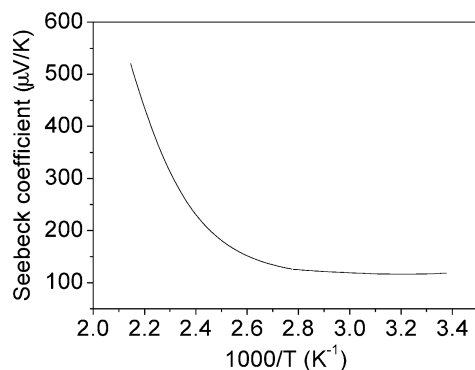


Fig. 10. Variation of Seebeck coefficient with temperature of a typical CuAlO₂ film on glass substrate.

value of the Seebeck coefficient was found to be $+128 \mu\text{V K}^{-1}$. Room temperature Hall effect measurement also indicated positive value of the Hall coefficient with a value $R_H = +16.7 \text{ cm}^3 \text{ C}^{-1}$, which corresponds to acceptor density $3.7 \times 10^{17} \text{ cm}^{-3}$. Thus, p-type conduction taking place in the films was confirmed from both TEP and Hall effect studies. It is believed that the excess oxygen, which was achieved by post-deposition annealing in oxygen atmosphere, is the reason for origin of p-type conduction in CuAlO₂ films, as suggested by Eq. (1).

4. Conclusion

Polycrystalline p-type semiconducting CuAlO₂ thin films were deposited by DC sputtering of sintered CuAlO₂ powder on Si and glass substrates successfully. XRD spectrum confirms the polycrystalline nature of the films with small grain size ($\sim 26 \text{ nm}$). The films were transparent in the visible region. P-type conductivity was confirmed from both TEP and Hall effect measurement. Sputtered-deposited transparent p-type semiconducting CuAlO₂ thin film showed a high room temperature conductivity of the order of 0.08 S cm^{-1} . Both allowed direct and indirect transitions were found to exist and the corresponding band gaps were determined to be 3.66 and 2.1 eV, respectively. FTIR spectra of the film indicated the existence of various bonding among Cu, Al and oxygen.

Acknowledgments

Two of the authors (A.N.B.) and (S.K.) wish to thank Council of Scientific and Industrial Research (CSIR), Government of India, for awarding them junior research fellowship (JRF) during the work.

References

- [1] I. Hamberg, C.G. Granqvist, *J. Appl. Phys.* 60 (1986) R123.
- [2] K.L. Chopra, S. Major, D.K. Pandya, *Thin Solid Films* 102 (1983) 1.
- [3] H. Cachet, A. Gamard, G. Campet, B. Jousseume, T. Toupance, *Thin Solid Films* 388 (2001) 41.
- [4] R. Wendt, K. Ellmer, *Surf. Coat. Technol.* 93 (1997) 27.
- [5] H. Kawazoe, M. Yasukawa, H. Hyodo, M. Kurita, H. Yanagi, H. Hosono, *Nature* 389 (1997) 939.
- [6] N. Duan, A.W. Sleight, M.K. Jayaraj, J. Tate, *Appl. Phys. Lett.* 77 (2000) 1325.
- [7] M.K. Jayaraj, A.D. Draeseke, J. Tate, A.W. Sleight, *Thin Solid Films* 397 (2001) 244.
- [8] H. Yanagi, H. Kawazoe, A. Kudo, M. Yasukawa, H. Hosono, *J. Electroceram.* 4 (2000) 427.
- [9] R. Nagarajan, A.D. Draeseke, A.W. Sleight, J. Tate, *J. Appl. Phys.* 89 (2001) 8022.
- [10] G. Thomas, *Nature* 389 (1997) 907.

- [11] K. Koumoto, H. Koduka, W.S. Seo, *J. Mater. Chem.* 11 (2001) 251.
- [12] A. Kudo, H. Yanagi, H. Hosono, H. Kawazoe, *Appl. Phys. Lett.* 73 (1998) 220.
- [13] A. Kudo, H. Yanagi, K. Ueda, H. Hosono, H. Kawazoe, Y. Yano, *Appl. Phys. Lett.* 75 (1999) 2851.
- [14] H. Kawazoe, H. Yanagi, K. Ueda, H. Hosono, *MRS Bull.* August (2000) 28.
- [15] C.F. Windisch Jr., K.F. Ferris, G.J. Exarhos, *J. Vac. Sci. Technol. A* 19 (2001) 1647.
- [16] C.F. Windisch Jr., G.J. Exarhos, K.F. Ferris, M.H. Engelhard, D.C. Stewart, *Thin Solid Films* 398–399 (2001) 45.
- [17] T. Ishiguro, N. Ishizawa, N. Mizutani, M. Kato, *J. Solid State Chem.* 41 (1982) 132.
- [18] Nonstoichiometry, Diffusion, and Electrical Conductivity in Binary Metal Oxides, Per Kofstad, Wiley–Interscience, 1972.
- [19] H. Yanagi, S. Inoue, K. Ueda, H. Kawazoe, H. Hosono, N. Hamada, *J. Appl. Phys.* 88 (2000) 4159.
- [20] JCPDS Powder Diffraction File Card 9–185.
- [21] S.B. Quadri, E.F. Skelton, D. Hsu, A.D. Dinsmore, J. Yang, H.F. Gray, B.R. Ratna, *Phys. Rev. B* 60 (1999) 9191.
- [22] *Infrared Spectra of Inorganic and Coordinated Compounds*, Nakamoto, John Wiley Sons, Inc., 1963.
- [23] P. Trate, *Spectrochim. Acta, Part A* 23 (1967) 2127.
- [24] F. Demichelis, G. Kaniadakis, A. Tagliaferro, E. Tresso, *Appl. Opt.* 26 (1987) 1737.
- [25] *Optical Processes in Semiconductors*, Pankove, Prentice-Hall, Inc., 1971.